

# Accelerated skin wound healing using electrospun nanofibrous mats blended with mussel adhesive protein and polycaprolactone

Bum Jin Kim,<sup>1</sup> Hokyun Cheong,<sup>1</sup> Eun-Som Choi,<sup>2</sup> So-Hee Yun,<sup>2</sup> Bong-Hyuk Choi,<sup>1</sup> Ki-Soo Park,<sup>2</sup> Ick Soo Kim,<sup>3</sup> Dae-Hwan Park,<sup>2</sup> Hyung Joon Cha<sup>1</sup>

<sup>1</sup>Department of Chemical Engineering, Pohang University of Science and Technology, Pohang 790-784, Korea

<sup>2</sup>Department of Plastic and Reconstructive Surgery, Daegu Catholic University Medical Center, Daegu 705-718, Korea

<sup>3</sup>Nano Fusion Technology Research Group, Division of Frontier Fibers, Institute for Fiber Engineering, Interdisciplinary Cluster for Cutting Edge Research, Shinshu University, Ueda 386-8567, Japan

Received 4 March 2016; revised 12 June 2016; accepted 14 September 2016

Published online 11 October 2016 in Wiley Online Library (wileyonlinelibrary.com). DOI: 10.1002/jbm.a.35903

**Abstract:** Nanofibrous scaffolds have been assessed as one of many promising tissue engineering scaffolds to be utilized for wound-healing applications. Previously, we reported multifunctionalized electrospun nanofibrous scaffolds blended with mussel adhesive protein (MAP) and polycaprolactone (PCL), which provide durable mechanical strength, cell-friendly environments, and a substantial ability to capture diverse bioactive molecules without any surface modifications. In the present work, we applied the blended nanofibrous mats of MAP and PCL for *in vivo* skin wound healing. The nanofibrous mats showed accelerated regeneration in a rat skin wound-healing model, which might be attributed to a highly compatible

environment for keratinocyte cell growth, an ability to capture inherent growth factors, and an efficient exudate absorption capacity. Thus, this work would suggest that adhesive property of scaffold could be a factor of successful application for wound healing. The MAP-blended nanofibers could also be potentially exploited for diverse tissue regeneration applications. © 2016 Wiley Periodicals, Inc. *J Biomed Mater Res Part A*: 105A: 218–225, 2017.

**Key Words:** mussel adhesive protein, nanofibrous mat, wound healing, skin regeneration, electrospinning

**How to cite this article:** Kim BJ, Cheong H, Choi E-S, Yun S-H, Choi B-H, Park K-S, Kim IS, Park D-H, Cha HJ. 2017. Accelerated skin wound healing using electrospun nanofibrous mats blended with mussel adhesive protein and polycaprolactone. *J Biomed Mater Res Part A* 2017;105A:218–225.

## INTRODUCTION

Skin is the largest organ in the human body, and it serves as an important role as a barrier protecting against external environments. Chronic or acute wounds can cause severe damage to the skin in spite of its capacity to form a self-renewing and self-healing interface between our body and the environment.<sup>1</sup> To treat various types of wounds, autologous skin grafting has been conventionally and widely applied. However, this procedure can be painful and can generate severe scar formation at donor sites. Recently, tissue engineered skin substitutes have been greatly recognized as an alternative treatment for wound healing. Because the wound-healing process is highly complicated and requires multiple steps, which should be sophisticatedly regulated by various types of cytokines and cells, many studies have attempted to understand the wound-healing process and promote skin regeneration via diverse tissue engineering strategies.<sup>2</sup>

Nanofibrous scaffolds that have structures similar to that of the actual extracellular matrix (ECM) have emerged

as an ideal scaffold type. Nanofibrous structures can be easily produced by a typical electrospinning process using diverse types of synthetic and natural polymers. Additionally, due to distinguishing characteristics, including high surface-to-volume ratio, fiber diameters ranging from tens to hundreds of nanometers, and high porosity and interconnectivity, electrospun nanofibers have been assessed as useful platforms for designing functional tissue engineering scaffolds.<sup>3–5</sup> Moreover, their characteristics of allowing gaseous and fluidic exchanges, absorbing excess exudates and wound odor, and offering biocompatible surface environments for cell adhesion and growth have been believed as suitable for wound-healing applications.<sup>6</sup>

As a component of electrospun nanofibers, synthetic polymers such as polycaprolactone (PCL) and poly(L-lactic acid-co-glycolic acid) (PLGA) have been considered as attractive materials due to their good spinnability and versatile mechanical performance.<sup>7</sup> However, the lack of a cell-recognition motif in synthetic polymer-based electrospun nanofibers has limited their biomedical applications. Thus,

**Correspondence to:** H. J. Cha; e-mail: hjcha@postech.ac.kr

Contract grant sponsor: Marine Biomaterials Research Center grant from Marine Biotechnology Program funded by the Ministry of Oceans and Fisheries, Korea

introduction of various types of bioactive substances into synthetic polymer-based nanofibers has been performed to enhance bioactive functionalities.<sup>8</sup> However, most of the previous methods are based on surface modification procedures that require multiple steps, harmful reagents, and highly skilled expertise.<sup>8</sup>

Mussel adhesive proteins (MAPs), which are secreted from mussel basal threads, have been assessed as key molecules of strong underwater mussel adhesion.<sup>9</sup> Additionally, MAPs have been considered as potential adhesive biomaterials due to their low immunogenicity in the human body, as well as their biocompatibility and biodegradability.<sup>9–12</sup> Moreover, high production and versatile modification of the MAPs via recombinant DNA technology and bacterial expression systems have provided the opportunities to exploit MAPs as biomaterials for applications in diverse fields.<sup>10,13–22</sup> Previously, mussel-inspired, multi-functional nanofibrous scaffolds based on recombinant MAPs have been reported, and their reinforced mechanical strength, biocompatibility, and sticky surface properties useful for the facile introduction of diverse biomolecules have gained much attention for potential applications in functional tissue engineering scaffolds.<sup>23,24</sup> In the present work, we evaluated the potency of the MAP-blended nanofibers as a functional wound healing material by investigating *in vivo* skin regeneration in a rat wound-healing model, which was subsequently supported *in vitro* by the identification of keratinocyte cell proliferation and growth factor capturing.

## MATERIALS AND METHODS

### Preparation of recombinant MAP

Recombinant hybrid MAP, fp-151, was expressed and purified as previously described.<sup>16</sup> In brief, recombinant *Escherichia coli* cells were cultured in 7 L of Luria-Bertani (LB) medium supplemented with 50 mg mL<sup>-1</sup> ampicillin (Sigma, St. Louis, MO) with a 10-L bioreactor (KoBiotech, Incheon, Korea) at 37°C and 250 rpm. At an optical density at 600 nm (OD<sub>600</sub>) of 0.5–0.8, 1 mM (final concentration) isopropyl-β-D-thiogalactopyranoside (IPTG; Sigma) was added to the culture medium to induce MAP expression, and the broth was further cultured for 8 h at 37°C and 250 rpm. After centrifuging the culture broth at 18,000g for 10 min at 4°C, cell pellets containing recombinant MAP were resuspended in 5 mL of lysis buffer (10 mM Tris-HCl and 100 mM sodium phosphate; pH 8.0) per gram wet weight. The resuspended cells were lysed with a constant cell disruption system (Constant Systems, Daventry, UK) at 20 kpsi. The lysates were centrifuged at 18,000g for 20 min at 4°C, and the inclusion bodies containing expressed MAP were collected for purification. The inclusion bodies were resuspended in 25% (v/v) acetic acid to extract the recombinant MAP. The extracted solution was centrifuged at 18,000g for 20 min at 4°C, and the supernatant was collected and freeze-dried.

### Fabrication of MAP-blended nanofibrous mats

The electrospinning process was carried out as described in a previous study.<sup>23</sup> Each polymer solution was prepared by dissolving PCL (Sigma) or MAP at a concentration of 6 wt %

in 1,1,1,3,3,3-hexafluoroisopropanol (HFIP; Sigma). The PCL solution was blended to produce a series of PCL/MAP solutions with different ratios of MAP concentrations including 0, 25, and 75 wt %. The blended solution was electrospun using a 5-mL syringe with a needle diameter of 0.4 mm and mass flow rate of 1 mL h<sup>-1</sup>. High voltage (13–15 kV) was applied to the tip of the needle attached to the syringe when the fluid jet was ejected. The nanofibers were collected on an aluminum foil with a gap distance of 10 cm from the needle tip. All of the electrospun nanofibers were vacuum-dried for at least 5 days to allow evaporation of any remaining solvent prior to use. The morphology of the nanofibers was analyzed using a scanning electron microscope (SEM; JSM-7401F; JEOL, Seoul, Korea) at an accelerating voltage of 5 kV. The nanofibers were sputtered with gold before observation. The mean nanofiber diameters were evaluated using image analysis software (Image J; NIH, Bethesda, MD).

### *In vivo* rat wound healing using MAP-blended nanofibrous mats

Male Sprague Dawley (SD) rats at 7 weeks of age were anesthetized with an intra-muscular injection of Zoletil (0.1 mL/100 g) and Rompun (0.04 mL/100 g). After shaving, two incisional, full-thickness circular wounds (2 cm in diameter) were made on the upper back of each animal using a sterile surgical scalpel. Areas equal to the wound sizes were treated with either control (untreated wound) or PCL or PCL/MAP (25:75) nanofibrous mats. Antiseptic gauze infiltrated with ampicillin was placed on each fibrous mat, and edges were sutured to the skin around the wound area after wrapping the gauze with Medifoam dressings (Mundipharma, Seoul, Korea). After anesthesia recovery, the animals were placed in individual cages and observed throughout the experiment. The Medifoam dressings were exchanged every 3 days.

On days 3, 8, 12, 17, and 21 post-surgery, the animals were sacrificed in a carbon dioxide chamber. For macroscopic evaluation of skin regeneration, the wounds were scanned after molding, and actual wound area was measured using ImageJ. For histological examination, hematoxylin and eosin (H&E) staining was carried out. Cryosections of the wounds were fixed into 4% formaldehyde and washed with distilled water; cell nuclei were stained with hematoxylin (Sigma), and then the sections were rinsed under running tap water; differentiated with 0.3% acid alcohol, rinsed in running tap water again, stained with eosin (Sigma) for 2 min, dehydrated, cleared and mounted. The H&E-stained sections were observed using a light microscope (Leica, Wetzlar, Germany).

### *In vitro* human keratinocyte culture on MAP-blended nanofibrous mats

The electrospun nanofibers were exposed to UV irradiation for 2 h and washed three times with phosphate-buffered saline (PBS) for 30 min each before cell seeding. The human keratinocyte cell line, HaCaT, was maintained in Dulbecco's modified Eagle's medium (DMEM; HyClone, Logan, UT) supplemented with 10% fetal bovine serum (FBS; HyClone) and 1% penicillin/streptomycin (HyClone) at 37°C in a

humidified atmosphere of 5% CO<sub>2</sub> and 95% air. Subconfluent cells were detached by 0.25% trypsin-EDTA (HyClone), and the viable cells were counted using trypan blue. The cells were further seeded onto PCL and PCL/MAP (75:25) nanofibrous mats that were placed in a 24-well plate, at a density of  $3 \times 10^4$  cells per well, and they were then cultured for further analysis. The morphology of the cells on each electrospun nanofiber mat was observed using SEM after 30 min and 4 days of cell culture in medium containing serum. The samples were fixed with 4% formaldehyde for 30 min and vacuum-dried; they were then sputtered with gold for observation of cell morphology. To assess cell proliferation on each nanofiber mat, cell viabilities were determined using a CCK-8 assay (Dojindo, Kumamoto, Japan). After each time point after cell seeding in 24-well plates, CCK-8 solutions were applied to each well and incubated for 2 h. The solution color changes were used to measure absorbance at 450 nm.

### QCM analysis

A quartz crystal microbalance (QCM; Stanford Research Systems, Sunnyvale, CA) was used to measure the binding of basic fibroblast growth factor (bFGF; R&D systems, Minneapolis, MN, USA) to the PCL and PCL/MAP (75:25) nanofibrous mats *in situ*. Before measurement of bFGF binding to the nanofibers, the same amount of each polymer solution was directly electrospun onto the quartz crystals. The flow was controlled by a syringe pump (WPI, Hertfordshire, UK) equipped with a low-pressure liquid chromatography injector valve and a 0.25-mL injection loop (Upchurch Scientific, Oak Harbor, WA). In each experiment, the nanofiber-mounted quartz crystal, with a resonant frequency of 5 MHz and an active area of 1.267 cm<sup>2</sup>, was first equilibrated with PBS in a 0.15-mL flow cell. Then, the target bFGF solution (250 ng mL<sup>-1</sup>) in PBS was loaded into a 0.25 mL-loop, injected, and allowed to flow through the flow cell containing a quartz crystal. After sufficient coating of bFGF and observation of a maintained equilibrium, PBS solution was flowed through the system to rinse the flow cell.

### Quantification of ability to capture growth factors

To quantitatively measure the capturing efficiency of bFGF onto each nanofiber, a fluorescein isothiocyanate (FITC)-labeling technique was used by following the manufacturer's instruction for FluoroTag<sup>TM</sup> (Sigma). FITC was dissolved in 0.1 M sodium bicarbonate buffer (pH 9.0), and the FITC solution was allowed to react with bFGF at room temperature for 2 h at a molar ratio of 50:1. FITC-labeled bFGF (F-bFGF) was separated from the FITC solution via flowing through a Sephadex G-25M column (Sigma).

PCL and PCL/MAP (75:25) nanofibrous mats 5 mm in diameter were placed in wells of a 48-well plate. An aliquot of 0.1 mL of 500 ng mL<sup>-1</sup> F-bFGF solution in PBS was added into each well. F-bFGF concentrations were determined by a bFGF Quantikine ELISA kit (R&D systems). After removing internally trapped air by decompression, the nanofibrous mats were incubated in the F-bFGF solution for 30 min at room temperature on a shaker. The supernatants

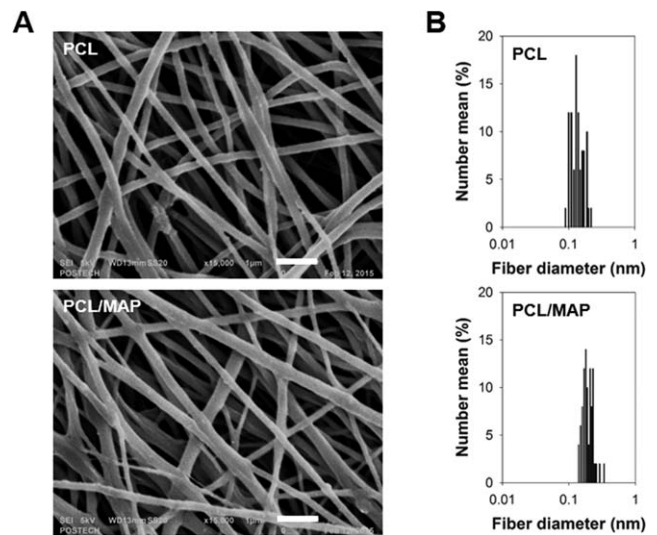


**FIGURE 1.** (A) SEM images and (B) fiber diameter distribution of PCL and PCL/MAP nanofibers. Scale bar is 1 μm.

were collected after washing the F-bFGF-bound mats with PBS twice. The amount of F-bFGF was determined by measuring the fluorescence intensity of each solution using a multi-well fluorescence spectrophotometer (Perkin Elmer, Waltham, MA, USA). Standard curves of F-bFGF were obtained using known concentrations of F-bFGF. The binding efficiency of F-bFGF to the nanofibrous mats was evaluated according to the following formula: binding efficiency (%) =  $[(W_a - W_b)/W_a] \times 100$ , where  $W_a$  and  $W_b$  represent the concentration of bFGF in PBS solution before and after incubation with the nanofibrous mats, respectively.

## RESULTS AND DISCUSSION

### Fabrication of MAP-blended nanofibrous mats

PCL and PCL/MAP nanofibrous mats were fabricated using typical electrospinning procedures, as previously reported.<sup>23</sup> PCL was selected as a blending partner with MAP for the fabrication of composite nanofibers because blended solutions of PCL and MAP showed stable spinnability for producing electrospun nanofibers compared with other types of synthetic polymers, and the nanofibers showed durable mechanical strength applicable to actual tissue experiments.<sup>23</sup> Through electrospinning, fine nanofibrous structures with fibers ~100–200 nm in diameter were obtained, as determined via SEM analysis (Fig. 1); these results are consistent with the results of our previous work.<sup>23</sup>

### *In vivo* wound healing of rat skin using MAP-blended nanofibrous mats

To assess the *in vivo* skin regeneration ability of the MAP-blended nanofibers, a rat full-thickness wound-healing model was used. To demonstrate functionalities of nanofibrous scaffolds composed of newly-developed biomaterials, synthetic polymers have been widely utilized as a backbone of the nanofibers.<sup>25</sup> Although lack of bioactive motifs needs to be overcome in the synthetic polymer-based nanofibers, their outstanding mechanical properties have been

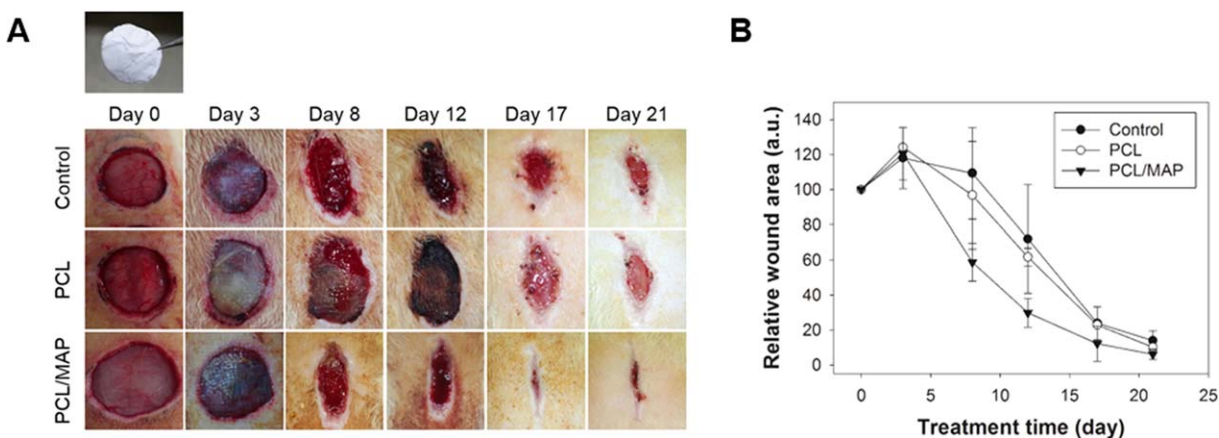


**FIGURE 2.** *In vivo* wound healing of rat skin after treatments with control (untreated wound) and PCL and PCL/MAP nanofibrous mats ( $n = 6$ ). (A) Macroscopic observation of wounds and (B) measured wound areas after treatment.

considered as a strong advantage for successful wound-healing applications. Therefore, in this study, comparative analyses among the control, PCL, and PCL/MAP nanofibers were performed to evaluate the role of the MAP component of the nanofibers during the wound-healing process. We qualitatively observed that the PCL/MAP mats showed an excellent capacity for absorbing exudates around the wound area and attaching closely to the wound surface, which might be attributed to the adhesive property of MAP. This adhesive ability of MAP-blended nanofibers would be a great advantage for handling and applying the mats to wound areas where copious amounts of blood and exudates are generated. Additionally, we clearly observed that wounds treated with PCL/MAP nanofibrous mats healed faster than wounds treated with PCL mats or not treated (control) [Fig. 2(A)]. At day 8 after treatment with the PCL/MAP nanofibrous mat, some granulation and a small amount of scab formation were observed on the skin surfaces, and highly regenerated epidermis covered the surrounding wounds. In the case of solely PCL nanofibrous mats, scab formation and limited granulation were observed. At day 12 after treatment, rigid membrane congestion caused by clotting and scabs was observed in the PCL group, which might have had an inhibitory effect on surrounding skin regeneration. Shriveling of the epithelium was observed, and the wounds were mostly filled with regenerated skin with hair growth in the PCL/MAP group at day 17. Meanwhile, rough, thin skin and limited regenerated epithelium were detected in the control and PCL groups until day 17. The wound images were analyzed to quantify the wound-healing area of each experimental group at different time points. An initial acceleration of wound healing was detected in the PCL/MAP nanofibrous mat group at day 8, and the differences of wound area between the PCL/MAP group and the other experimental groups were remarkable after treatment for 12 days [Fig. 2(B)]. Additionally, at the final stage of regeneration, the most recovered wound areas were detectable in the PCL/MAP group. Given that natural wound closure of normal rat skin can be mostly completed within 3–4 weeks, it is recognizable that wound-healing rate

was improved by the PCL/MAP nanofiber at 1–2 weeks comparing with the nontreated and PCL nanofiber-treated groups in normal rats. It would be also worth applying the PCL/MAP nanofiber for regeneration of diseased models such as a diabetic rat model in order to identify advanced functionalities of MAP for further applications.

Through analyses of magnified H&E staining images, we could approximately determine the status of skin regeneration [Fig. 3(A)]. At week 3 after treatment, the final week, newly formed, normal skin tissues had been generated in most of the wound areas, and keratinocyte layers were tightly formed on the outer surface of the wounds in the PCL/MAP group. However, wounds in the PCL group showed remaining abrasions and granulations in large central areas of the wounds. Proper ECM remodeling requires the removal of granulation tissue and revascularization, which provides nutrients for tissue regeneration and favorable conditions for epithelium growth.<sup>6</sup> Figure 3(B) shows angiogenesis and tissue formation in the endodermis area of each experimental group at weeks 2 and 3 after treatment. The maturation of keratinocytes and formation basal layers of the wounds in the PCL/MAP group seemed to have progressed well at weeks 2 and 3 after treatment. However, deficient keratinocyte and basal layer formation and remaining wounds were detected in the PCL group.

On the basis of the *in vivo* experimental results, we surmised that the enhanced wound healing facilitated by the MAP-blended nanofibers would be due in large part to substrate properties favorable for cell adhesion and growth as well as for recruiting inherent bioactive molecules such as growth factors. Therefore, we next evaluated keratinocyte cell behavior and growth factor capturing *in vitro* to provide evidence of the contribution of MAP in the promotion of the wound-healing process.

#### ***In vitro* human keratinocyte cell behavior on MAP-blended nanofibers**

To investigate whether MAP-blended nanofibers are biocompatible and provide a cell-friendly environment, an *in vitro* keratinocyte culture study was performed. Keratinocyte cells

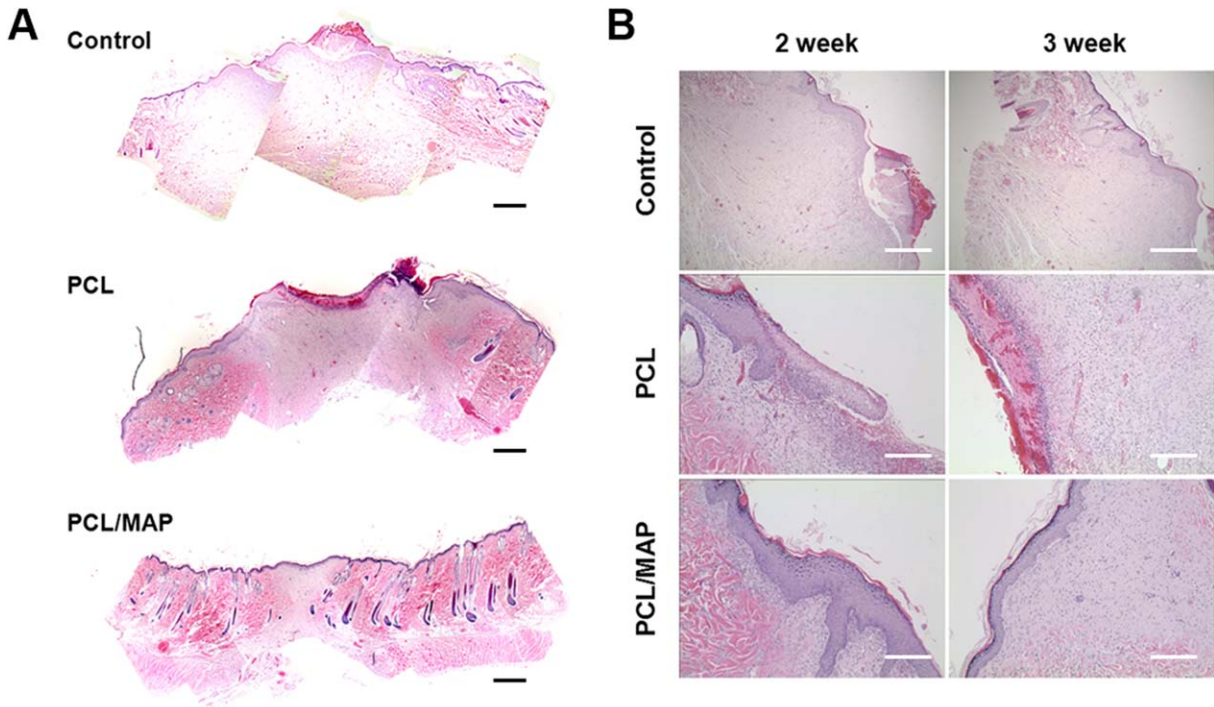


**FIGURE 3.** Histological analyses of wound areas after treatments with control (untreated wound) and PCL and PCL/MAP nanofibrous mats ( $n = 6$ ). (A) H&E staining of entire wound areas at 3 weeks after treatment. Scale bar is 1 mm. (B) H&E staining of basal layers of wound areas at 2 and 3 weeks after treatment. Scale bar is 200  $\mu\text{m}$ .

cultured on PCL and PCL/MAP nanofibers for 30 min and 4 days were observed via SEM to assess cell population and morphology. The cells on the PCL/MAP nanofibers were more spread after the initial 30 min of adhesion and occupied more area than did cells on the PCL nanofibers after 4 days of culture [Fig. 4(A)]. Those cell growth profiles were evaluated using a cell viability assay. We detected a higher degree of cell growth on the PCL/MAP nanofibers than on the PCL nanofibers [Fig. 4(B)], which was consistent with the SEM analysis. A physical attraction to MAP as well as the hydrophilicity of the MAP-blended nanofiber surface might provide favorable environments for the effective

adhesion and growth of keratinocyte cells. Thus, the higher degree of basal layer maturation and the subsequent acceleration of skin regeneration in wounds of the PCL/MAP nanofiber-treated group could be explained by the higher keratinocyte growth rate on the MAP-blended nanofibers *in vitro*.

Keratinocytes, which can be formed by the differentiation of epidermal stem cells residing in the basal layer of the epidermis, play an important role in wound healing via migrating to fill wound gaps, contributing hair follicle formation, and protecting wounds from external environments.<sup>26–28</sup> Additionally, as an *in vitro* model, investigating

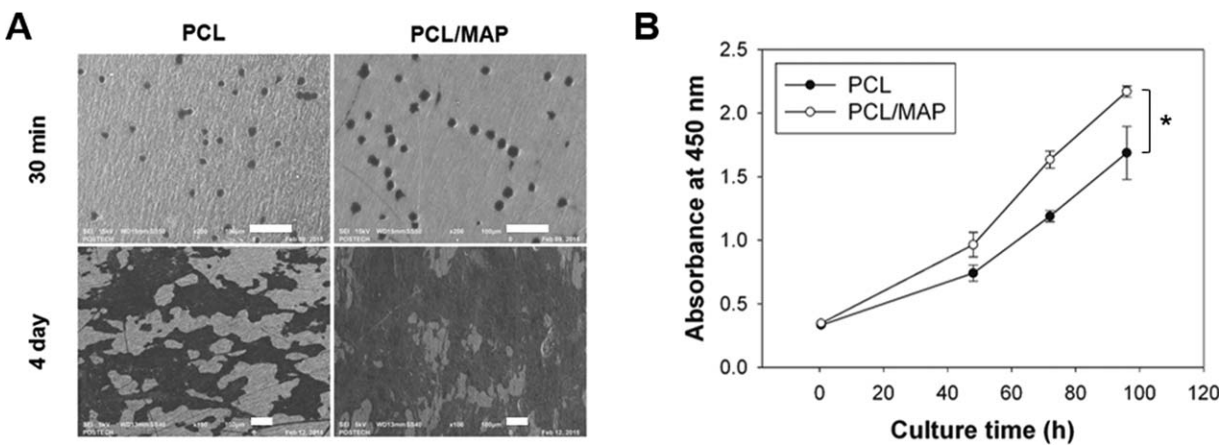


**FIGURE 4.** *In vitro* keratinocyte cell behaviors on nanofibrous mats. (A) SEM images and (B) viability profiles of keratinocytes on PCL and PCL/MAP nanofibers. Scale bar is 100  $\mu\text{m}$ . The cell viability experiment was performed in triplicate ( $*p < 0.05$ ).

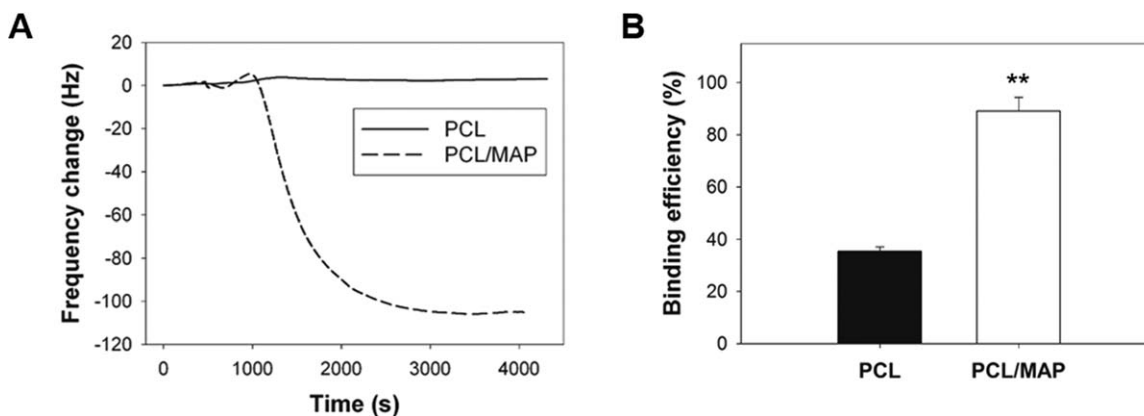


**FIGURE 5.** Capturing ability of nanofibers against bFGF. (A) QCM analyses after injection of bFGF solution on gold electrode surfaces covered with PCL and PCL/MAP nanofibers. (B) Quantification of bFGF binding efficiency using F-bFGF on PCL and PCL/MAP nanofibers. The experiment was performed in triplicate (\*\* $p < 0.01$ ).

keratinocyte behavior has been exploited to identify the feasibility of electrospun nanofibrous scaffolds as wound-healing materials.<sup>29–33</sup> Biodegradable synthetic polymers such as PCL, poly(hydroxybutyrate) (PHB), and poly(lactic acid) (PLA) have been used as backbone polymeric materials for culturing keratinocytes. However, it seems to be necessary to apply additional bioactive molecules for the acceleration of keratinocyte adhesion and growth. The additions of epidermal growth factor (EGF) as well as natural biopolymers, including gelatin, hyaluronan, and chitosan, have been assessed as appropriate components to incorporate into those synthetic polymers.<sup>29–33</sup>

#### MAP-blended nanofiber ability to capture growth factors

To assess the performance of the MAP-blended nanofibers in capturing growth factors, simple coating experiments were conducted. It has already been reported that MAP-blended nanofibers showed a recognizable ability to capture proteins, nucleic acids, and carbohydrates.<sup>23</sup> In this study, we observed a similar tendency for the capture of growth factors. We analyzed changes in frequency as a function of

time after injection of the bFGF solution into the flow cell containing a nanofiber-mounted quartz crystal [Fig. 5(A)]. The frequency change for the PCL nanofiber-mounted surface was negligible over time, indicating that the mass change due to bFGF binding was undetectable. Meanwhile, we detected dramatically decreased frequency by the injection of bFGF solution into the flow cell containing a PCL/MAP nanofiber-mounted quartz crystal. bFGF binding on the PCL/MAP nanofiber surfaces was achieved rapidly in 5 min, and detachment of bFGF did not occur with continuous flow of PBS solution.

To quantify the precise binding efficiency of bFGF on the nanofibers, FITC conjugation of bFGF was carried out to measure the fluorescence intensity of FITC-conjugated bFGF (F-bFGF) instead of direct bFGF quantification. The binding efficiencies of bFGF on the PCL and PCL/MAP nanofibers were determined and compared [Fig. 5(B)]. It was observed that the binding efficiency of bFGF on the PCL/MAP nanofibers was more than two times higher than that on the PCL nanofibers. Synthetic hydrophobic polymer-based scaffolds seem to have negligible capturing capacity due to the absence of functional groups for capturing. In contrast,

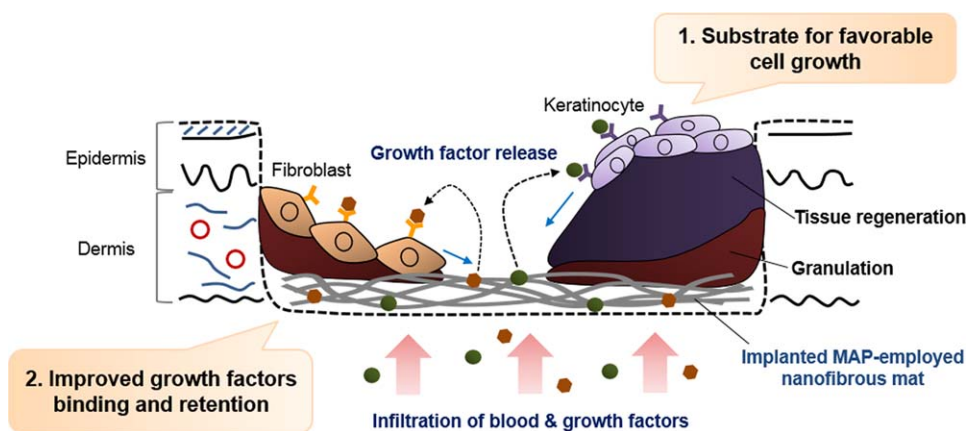


**FIGURE 6.** Schematic illustration of suggested mechanisms for enhanced *in vivo* rat skin regeneration where MAP-blended nanofibrous mats were used. Highly compatible environments for keratinocyte cell growth, substantial ability to capture inherent growth factors, and efficient exudate absorption capacity could collectively be possible explanations for accelerated skin regeneration.

MAP-blended nanofibers have accessible sticky MAP molecules and showed a substantial ability for capturing growth factors, which might be due to the charged amino acid residue-mediated hydrogen bonding, electrostatic interactions, and cation- $\pi$  and  $\pi$ - $\pi$  interactions of MAPs.<sup>12,34,35</sup> In particular, given the charge property similarity between bFGF and MAP (both pI values are  $\sim 10$ ), the substantial adhesive property of MAP might be involved in this molecular interaction between them. In addition, we could not find any capturing efficiency differences, even using bFGF coating solutions of concentrations five times higher (data not shown). This result demonstrates that the maximal amount of bFGF can be incorporated into the MAP-based nanofibers by a simple dipping procedure using a high concentration of the target bFGF solution. This type of capturing method exploiting the adhesive properties of MAPs could be advantageous compared with conventional surface modification procedures, which require relatively complicated steps.<sup>8</sup>

Growth factors are destined to transmit signals stimulating or inhibiting cellular proliferation, differentiation, and ECM secretion. In particular, bFGF is a multifunctional growth factor that promotes the growth and differentiation of a broad spectrum of cell types, including dermal fibroblasts, keratinocytes, endothelial cells, and melanocytes, for wound healing.<sup>36</sup> In the proliferative phase of the wound-healing process, various types of growth factors and cytokines, including bFGF, are secreted for the active promotion of multiple steps, such as angiogenesis, granular tissue formation, and re-epithelialization.<sup>37</sup> Additionally, these growth factors play significant roles in the enhancement of the growth and differentiation of a broad spectrum of cell types participating in the wound-healing process.<sup>37</sup> From the perspective that growth factors are readily enzymatically digested or deactivated and normally bind to ECM molecules to activate and stabilize target cells, the immobilization of growth factors has been considered an important issue for proper skin regeneration.<sup>38</sup> Therefore, the substantial ability of the MAP-blended nanofibers to capture growth factors, which could also retain secreted growth factors around the nanofibrous mats, might be one explanation for the enhanced skin regeneration observed in wounds of the PCL/MAP nanofibrous mat-treated group.

## CONCLUSIONS

In this work, the MAP-blended nanofiber platform, which exhibited substantial adhesive properties from MAP on the surface of nanofibers produced by electrospinning simple synthetic polymer blends, was successfully applied for the acceleration of skin regeneration in an *in vivo* rat wound-healing model. We proposed that appropriate biological interactions that were favorable for skin regeneration occurred between the sticky surface of the MAP-blended nanofibrous mat and skin wound environment. This might be explained by the results of our *in vitro* comparative experiments with solely synthetic polymer nanofibrous mats. The hydrophilicity of the MAP-blended nanofibrous mat facilitated extensive keratinocyte spreading and rapid

growth, which would support enhanced cell/tissue infiltration and basal layer formation (Fig. 6). In addition, a capacity of the MAP-blended nanofibrous mat for growth factor entrapment three times higher would retain inherent growth factors in the wound area such that they could effectively activate adjacent cells and tissues and consequently improve skin regeneration (Fig. 6). Collectively, our study reinforced the idea that the adhesive property of nanomaterials could be a factor of successful wound-healing applications. Moreover, successful application of the MAP-blended nanofiber platform in our study will potentially provide opportunities not only for developing advanced functionalized nanofibers via introducing bioactive molecules such as growth factors and functional peptides but also for applying for regeneration of many other types of damaged tissues.

## REFERENCES

1. Clark RA, Ghosh K, Tonnesen MG. Tissue engineering for cutaneous wounds. *J Invest Dermatol* 2007;127:1018–1029.
2. Jayaraman K, Kotaki M, Zhang Y, Mo X, Ramakrishna S. Recent advances in polymer nanofibers. *J Nanosci Nanotechnol* 2004;4:52–65.
3. Baker BM, Handorf AM, Ionescu LC, Li WJ, Mauck RL. New directions in nanofibrous scaffolds for soft tissue engineering and regeneration. *Expert Rev Med Dev* 2009;6:515–532.
4. Barnes CP, Sell SA, Boland ED, Simpson DG, Bowlin GL. Nanofiber technology: Designing the next generation of tissue engineering scaffolds. *Adv Drug Deliv Rev* 2007;59:1413–1433.
5. Nisbet DR, Forsythe JS, Shen W, Finkelstein DI, Horne MK. Review paper: A review of the cellular response on electrospun nanofibers for tissue engineering. *J Biomater Appl* 2009;24:7–29.
6. Yang Y, Xia T, Zhi W, Wei L, Weng J, Zhang C, Li X. Promotion of skin regeneration in diabetic rats by electrospun core-sheath fibers loaded with basic fibroblast growth factor. *Biomaterials* 2011;32:4243–4254.
7. Liang D, Hsiao BS, Chu B. Functional electrospun nanofibrous scaffolds for biomedical applications. *Adv Drug Deliv Rev* 2007;59:1392–1412.
8. Yoo HS, Kim TG, Park TG. Surface-functionalized electrospun nanofibers for tissue engineering and drug delivery. *Adv Drug Deliv Rev* 2009;61:1033–1042.
9. Strausberg RL, Link RP. Protein-based medical adhesives. *Trends Biotechnol* 1990;8:53–57.
10. Cha HJ, Hwang DS, Lim S. Development of bioadhesives from marine mussels. *Biotechnol J* 2008;3:631–638.
11. Lee BP, Messersmith PB, Israelachvili JN, Waite JH. Mussel-inspired adhesives and coatings. *Annu Rev Mater Res* 2011;41:99–132.
12. Silverman HG, Roberto FF. Understanding marine mussel adhesion. *Mar Biotechnol (NY)* 2007;9:661–681.
13. Choi BH, Cheong H, Jo YK, Bahn SY, Seo JH, Cha HJ. Highly purified mussel adhesive protein to secure biosafety for *in vivo* applications. *Microb Cell Fact* 2014;13:52.
14. Choi B-H, Cheong H, Ahn J-S, Zhou C, Kwon JJ, Cha HJ, Jun SH. Engineered mussel biogel as a functional osteoinductive binder for grafting of bone substitute particles to accelerate *in vivo* bone regeneration. *J Mater Chem B* 2015;3:546–555.
15. Hong JM, Kim BJ, Shim JH, Kang KS, Kim KJ, Rhie JW, Cha HJ, Cho DW. Enhancement of bone regeneration through facile surface functionalization of solid freeform fabrication-based three-dimensional scaffolds using mussel adhesive proteins. *Acta Biomater* 2012;8:2578–2586.
16. Hwang DS, Gim Y, Yoo HJ, Cha HJ. Practical recombinant hybrid mussel bioadhesive fp-151. *Biomaterials* 2007;28:3560–3568.
17. Hwang DS, Kim KR, Lim S, Choi YS, Cha HJ. Recombinant mussel adhesive protein as a gene delivery material. *Biotechnol Bioeng* 2009;102:616–623.
18. Jeon EY, Hwang BH, Yang YJ, Kim BJ, Choi BH, Jung GY, Cha HJ. Rapidly light-activated surgical protein glue inspired by

- mussel adhesion and insect structural crosslinking. *Biomaterials* 2015;67:11–19.
19. Jo YK, Seo JH, Choi BH, Kim BJ, Shin HH, Hwang BH, Cha HJ. Surface-independent antibacterial coating using silver nanoparticle-generating engineered mussel glue. *ACS Appl Mater Interfaces* 2014;6:20242–20253.
  20. Kim BJ, Cheong H, Hwang BH, Cha HJ. Mussel-inspired protein nanoparticles containing iron(III)-DOPA complexes for pH-responsive drug delivery. *Angew Chem Int Ed Engl* 2015;54:7318–7322.
  21. Kim CS, Choi BH, Seo JH, Lim G, Cha HJ. Mussel adhesive protein-based whole cell array biosensor for detection of organophosphorus compounds. *Biosens Bioelectron* 2013;41:199–204.
  22. Kim HJ, Hwang BH, Lim S, Choi BH, Kang SH, Cha HJ. Mussel adhesion-employed water-immiscible fluid bioadhesive for urinary fistula sealing. *Biomaterials* 2015;72:104–111.
  23. Kim BJ, Choi YS, Cha HJ. Reinforced multifunctionalized nanofibrous scaffolds using mussel adhesive proteins. *Angew Chem Int Edit* 2012;51:675–678.
  24. Kim BJ, Kim S, Oh DX, Masic A, Cha HJ, Hwang DS. Mussel-inspired adhesive protein-based electrospun nanofibers reinforced by Fe(III)-DOPA complexation. *J Mater Chem B* 2014;3:112–118.
  25. Norouzi M, Boroujeni SM, Omidvarkordshouli N, Soleimani M. Advances in skin regeneration: Application of electrospun scaffolds. *Adv Healthc Mater* 2015;4:1114–1133.
  26. Houben E, De Paepe K, Rogiers V. A keratinocyte's course of life. *Skin Pharmacol Physiol* 2007;20:122–132.
  27. Ito M, Liu Y, Yang Z, Nguyen J, Liang F, Morris RJ, Cotsarelis G. Stem cells in the hair follicle bulge contribute to wound repair but not to homeostasis of the epidermis. *Nat Med* 2005;11:1351–1354.
  28. Myers SR, Leigh IM, Navsaria H. Epidermal repair results from activation of follicular and epidermal progenitor keratinocytes mediated by a growth factor cascade. *Wound Repair Regen* 2007;15:693–701.
  29. Asran A, Razghandi K, Aggarwal N, Michler GH, Groth T. Nanofibers from blends of polyvinyl alcohol and polyhydroxy butyrate as potential scaffold material for tissue engineering of skin. *Biomacromolecules* 2010;11:3413–3421.
  30. Feng B, Duan H, Fu W, Cao Y, Jie Zhang W, Zhang Y. Effect of inhomogeneity of the electrospun fibrous scaffolds of gelatin/polycaprolactone hybrid on cell proliferation. *J Biomed Mater Res A* 2015;103:431–438.
  31. Jang SI, Mok JY, Jeon IH, Park KH, Nguyen TT, Park JS, Hwang HM, Song MS, Lee D, Chai KY. Effect of electrospun non-woven mats of dibutyl chitin/poly(lactic acid) blends on wound healing in hairless mice. *Molecules* 2012;17:2992–3007.
  32. Sundaramurthi D, Krishnan UM, Sethuraman S. Biocompatibility of poly(3-hydroxybutyrate-co-3-hydroxyvalerate) (PHBV) nanofibers for skin tissue engineering. *J Biomed Nanotechnol* 2013;9:1383–1392.
  33. Wang Z, Qian Y, Li L, Pan L, Njunge LW, Dong L, Yang L. Evaluation of emulsion electrospun polycaprolactone/hyaluronan/epidermal growth factor nanofibrous scaffolds for wound healing. *J Biomater Appl* 2015;30:686–698.
  34. Hwang DS, Zeng H, Lu Q, Israelachvili J, Waite JH. Adhesion mechanism in a DOPA-deficient foot protein from green mussels. *Soft Matter* 2012;8:5640–5648.
  35. Waite JH. Reverse engineering of bioadhesion in marine mussels. *Ann N Y Acad Sci* 1999;875:301–309.
  36. Werner S, Grose R. Regulation of wound healing by growth factors and cytokines. *Physiol Rev* 2003;83:835–870.
  37. Williams ML, Bhatia SK. Engineering the extracellular matrix for clinical applications: Endoderm, mesoderm, and ectoderm. *Bio-technol J* 2014;9:337–347.
  38. Lee K, Silva EA, Mooney DJ. Growth factor delivery-based tissue engineering: General approaches and a review of recent developments. *J R Soc Interface* 2011;8:153–170.